



Evaluation of tumor shape features for overall survival prognosis in glioblastoma multiforme patients



Parita Sanghani^a, Ang Beng Ti^b, Nicolas Kon Kam King^b, Hongliang Ren^{a,*}

^a National University of Singapore, Singapore

^b National Neuroscience Institute, Singapore

ARTICLE INFO

Keywords:

Glioblastoma multiforme
Overall survival prognosis
Shape feature extraction

ABSTRACT

Glioblastoma multiforme (GBM) is a rapidly growing tumor associated with poor prognosis. This study evaluates the effectiveness of thirteen tumor shape features for overall survival (OS) prognosis in GBM patients. Shape features were extracted from the abnormality regions of the GBM tumor visible on the fluid attenuated inversion recovery (FLAIR) and T1-weighted contrast enhanced (T1CE) MR images of GBM patients. Survival analysis was performed using univariate and multivariate (with clinical features) Cox proportional hazards regression analysis. Kaplan-Meier survival curves were plotted and observed for the shape features which were found to be significant from the Cox regression analysis. Three 3D shape features: Bounding ellipsoid volume ratio (BEVR), sphericity and spherical disproportion, computed from both the abnormality regions were found to be significant for OS prognosis in GBM patients.

1. Introduction

Glioblastoma multiforme (GBM) is the most prevalent form of malignant brain tumors in adults. They are aggressive in nature, and are associated with poor prognosis. The median survival is around 12–15 months [1–3]. The poor prognosis is attributed to the molecular and genomic heterogeneity [4–6].

Magnetic resonance imaging (MRI) plays a vital role in neuro-oncology for diagnosis of GBM in patients and consequent surgical planning. The use of MR imaging has previously been limited to diagnosis and monitoring of the prescribed treatment response. However, several features extracted from pre-operative MR images (such as volumetric, texture and shape of the tumors) have been found to be correlated with overall survival (OS) [7–10].

The existing literature implies that the location of the tumor is effective in OS prediction [11,12]. Necrosis volume and necrosis-tumor volume ratio have been shown to be prognostic of OS [13]. Age, Karnofsky performance scale (KPS) score, extent of resection, and the degree of necrosis and enhancement of the tumor on preoperative MR imaging studies are five independent predictors of survival [1]. However, the role played by extent of resection in survival prediction has not yet been completely understood [14,15].

Along with the clinical, volumetric and texture features, certain shape features have been analyzed for their significance in OS prognosis

of GBM patients. Czarnek et al. have shown that the three dimensional (3D) shape feature, bounding ellipsoid volume ratio (BEVR), is significant for the same [7].

Pyradiomics, an open-source python library computes shape features like sphericity and spherical disproportion from clinical images [16]. However, these shape features have not been used for OS prognosis in GBM patients.

Some two dimensional (2D) shape features have been shown to be effective for tumor characterization in breast cancer patients [17]. However, these 2D shape features have not been tested for OS prognosis in GBM patients.

This work aims to evaluate 13 shape features (3D and 2D) for OS prognosis in GBM patients. Each shape feature is individually assessed using univariate Cox regression for survival analysis. The features found to be significant from the univariate analysis were then combined with clinical features (age and KPS) to perform multivariate Cox regression. Kaplan-Meier (KM) survival curves were plotted for the features found to be significant from both univariate and multivariate Cox regression analysis to illustrate the effectiveness of a feature in OS prognosis.

In this study, we evaluated and compared the shape features extracted from tumor abnormalities observed in both fluid attenuated inversion recovery (FLAIR) and T1-weighted contrast enhanced (T1CE) MR images as the FLAIR and T1CE abnormalities differ due to the presence of edema in the FLAIR abnormality, which changes the tumor

* Corresponding author.

E-mail address: ren@nus.edu.sg (H. Ren).

shape characteristics.

2. Materials and methods

2.1. Data

We performed our analysis on 75 GBM patients from the Brain Tumor Segmentation (BraTS) 2017 challenge dataset [18–21]. The BraTS dataset consists of multi-channel MR images: T1-weighted, T1-weighted contrast-enhanced (T1CE), T2-weighted and FLAIR. All the MR images of a subject were registered to its T1CE image which had the highest spatial resolution. Two sets of masks obtained from the segmentation labels of the BraTS 2017 dataset were analyzed. In this study, a mask is referred to as a binary image where the voxel values inside the region of interest (ROI) is 1 and 0 otherwise.

- **FLAIR Mask:** It consisted of the enhanced tumor, non-enhanced tumor, necrosis and edema region which appears bright in the FLAIR image.
- **T1CE Mask:** It consisted of the enhanced tumor, non-enhanced tumor and necrosis region which can be identified on the T1CE image.

Fig. 1 shows the FLAIR and T1CE masks and its constituents for a patient data obtained from the BraTS 2017 dataset.

2.2. Tumor shape features

Shape features quantify various aspects of the tumor shape - geometry and surface irregularities. These features provide information which can be useful for OS prognosis. Tumor shape features have been found to be prognostic of survival in GBM patients [7]. In this work, we derived shape features from three dimensional (3D) and two dimensional (2D) tumor masks.

2.2.1. 3D tumor shape features

2.2.1.1. Bounding ellipsoid volume ratio. Czarnek et al. have shown that the bounding ellipsoid volume ratio (BEVR) of tumor is significantly prognostic of OS in GBM patients [7]. BEVR is the ratio of the volume of the tumor to that of the volume of the minimum volume ellipsoid bounding the tumor. BEVR is an indicator of the irregularity of the tumor shape. A high BEVR value indicates that the tumor is has lesser irregularities and a low BEVR value indicates that the tumor has considerable irregularities. Fig. 2 illustrates the minimum volume bounding ellipsoid corresponding to the FLAIR and T1CE masks for two patients. In this work, the minimum volume ellipsoid bounding the 3D tumor¹ was computed as shown by Moshtagh [22].

2.2.1.2. Orientation of the bounding ellipsoid. The ellipsoid formulation in the 3D Cartesian coordinate system, $\mathbf{x} \in \mathbb{R}^3$ is given as $\mathbf{x}^T A \mathbf{x} = 0$ where $A \in \mathbb{R}^3$ and A is positive definite. The minimum volume bounding ellipsoid of the 3D tumor mask was obtained as described by Moshtagh [22]. The major, intermediate and minor axis orientation information can be computed from the left singular values of A of the obtained minimum volume bounding ellipsoid. The left singular value matrix (say U) was obtained from the singular value decomposition (SVD) of A as $A = USV^T$. The orientation of the axes in the three orthogonal directions, $\Theta = \{\omega, \epsilon, \psi\}$ were computed from the formulae [23] shown in Eq. (1). In Eq. (1), U_{ij} is the element in the i -th row and j -th column of matrix U .

¹ <https://www.mathworks.com/matlabcentral/fileexchange/9542-minimum-volume-enclosing-ellipsoid?requestedDomain=www.mathworks.com>.

$$\tan(\omega) = \frac{-U_{21}}{U_{11}}$$

$$\tan(\epsilon) = \frac{-U_{32}}{U_{33}} \tag{1}$$

$$\tan(\psi) = \frac{U_{31}}{\sqrt{U_{32}^2 + U_{33}^2}}$$

2.2.1.3. Spherical disproportion and sphericity. Spherical disproportion (S_d) is the ratio of the surface area of the tumor region to the surface area of a sphere with the same volume as the tumor region. Sphericity (S_p) is the inverse of S_d . These features measure the roundness of the tumor region with respect to a sphere. The formulation of S_d and S_p are shown in Eq. (2).

$$S_d = \frac{A}{\sqrt[3]{36\pi V^2}}$$

$$S_p = \frac{\sqrt[3]{36\pi V^2}}{A} \tag{2}$$

where R is the radius of a sphere with the same volume as the tumor, and is thus equal to $\sqrt[3]{3V/4\pi}$. From the formulations in Eq. (2), it can be observed that $S_d > 1$ and $S_p \in (0,1]$ for all cases. For a perfectly spherical object, both S_d and S_p will have a value of 1. A high value of S_p and low value of S_d indicates that the tumor is approximately spherical and hence, it has low irregularities. However, a low value of S_p and high value of S_d indicates that the tumor surface is considerably irregular. These features were computed using *pyradiomics*, an open-source python package for the extraction of radiomics features from medical images [16].

2.2.2. 2D shape features

Seven 2D shape features were investigated in this study for their effectiveness in survival prognosis of GBM patients, which have previously provided good characterization of the mammographic mass in breast cancer patients [17]. The 2D shape features were computed from the axial slice where the tumor occupied maximum area. To compute these features, the centroid of the 2D tumor mass was computed, followed by prototype edge-following method to acquire the tumor mass boundary. The starting point on the mass boundary was acquired at an arbitrary angle and was then registered in full resolution, using a line-following scheme. The radial distances between the centroid and the detected boundary pixels were calculated. All radial distances computed were normalized using the minimum and maximum values of radial distances in the dataset, in order to avoid excessive differences in magnitude and total energy between tumors of different sizes. The 2D shape features: mean radial distance (MRD), radial distance standard deviation (RDS), mass circularity (MC), entropy of radial distance (Entropy), area ratio (AR), zero crossing count (ZC) and mass boundary roughness (MBR) were calculated using the normalized radial distances as done by Georgiou et al. [17]. An irregular tumor will have higher values for radial distance standard deviation, zero crossing, mass boundary roughness, entropy, area ratio, but a lower circularity value as compared to a relatively regular shaped tumor. In this study, these features were employed as tumor shape descriptors for studying OS prognosis in GBM patients.

2.3. Statistical analysis

The effectiveness of the shape features for overall survival (OS) prognosis was assessed by performing Cox proportional hazard regression analysis.

2.3.1. Univariate Cox proportional hazard regression analysis

Significance of each shape feature for OS prognosis was obtained

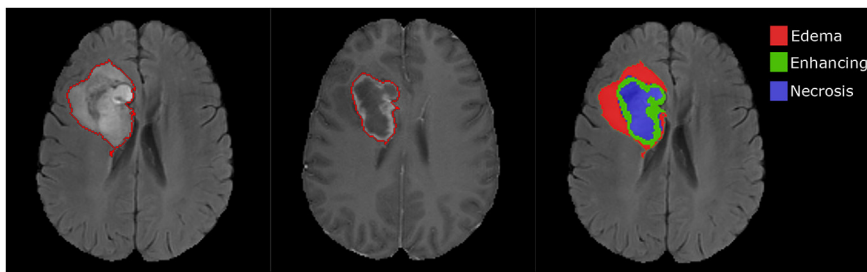
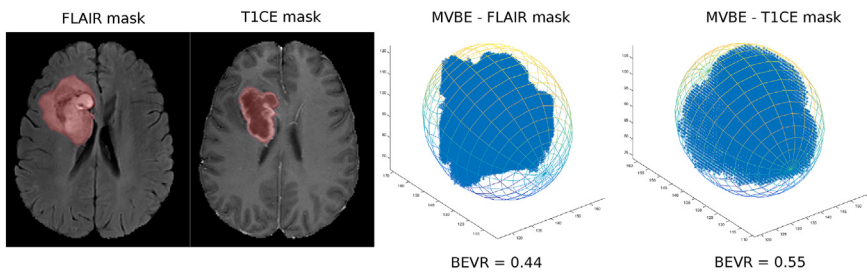
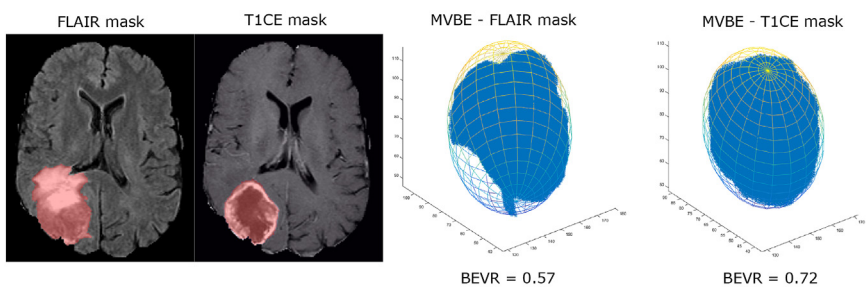


Fig. 1. (Left to Right) FLAIR MR image with FLAIR mask overlay. T1-weighted contrast-enhanced (T1CE) MR image with T1CE mask overlay. BraTS 2017 segmentation label overlay on FLAIR MR image showing the peritumoral edema (ED ROI), the contrast-enhanced tumor (ET ROI) and necrosis and non-enhancing tumor (NEC ROI). Patient ID: Brats17_TCIA_186_1.



(a) Patient ID: Brats17_TCIA_186_1



(b) Patient ID: Brats17_TCIA_335_1

Fig. 2. The minimum volume bounding ellipsoid (MVBE) of the FLAIR and T1CE masks are illustrated for two GBM patient cases: (a) Brats17_TCIA_186_1 and (b) Brats17_TCIA_335_1. (From left to right) FLAIR mask overlay on FLAIR MR image, T1CE mask overlay on T1CE MR image, MVBE computed from the FLAIR mask, MVBE computed from the T1CE mask. The MVBE figures for each mask is accompanied with their corresponding BEVR values.

from univariate Cox regression. Hazard ratios (HR) and its 95% confidence interval (CI) obtained from the univariate Cox regression analysis indicates the performance of the feature in OS prognosis of GBM patients. The p-value and Wald statistic value (w) were reported to determine the performance of the regression model.

2.3.2. Multivariate Cox proportional hazard regression analysis

The shape features found to be significant predictors of OS from the univariate analysis were analyzed using multivariate Cox regression. Two clinical variables: age and KPS were added as covariates to the multivariate regression model along with the significant shape features obtained from the univariate analysis.

The univariate and multivariate Cox regression analysis was performed using the Survival package (version 2.41–3) in R.

2.3.3. Kaplan-Meier curve analysis

Kaplan-Meier (KM) curves were obtained for the features that were found to be significant from both univariate and multivariate Cox regression analysis to illustrate the effectiveness of the features for OS prognosis in GBM patients.

3. Results

The mean and standard deviation of the features estimated for all the GBM patients considered in this study are shown in Table 1.

4. Discussion

Radiomics is an emerging field of research which involves

Table 1

The mean (μ) and standard deviation (σ) values of the 2D and 3D shape features computed from the FLAIR and T1CE masks of 75 GBM patients.

Features	μ		σ	
	FLAIR mask	T1CE mask	FLAIR mask	T1CE mask
Area Ratio	0.21	0.22	0.05	0.04
Mass Circularity	45.11	26.68	23.44	4.71
Entropy of radial distance	9.71	6.70	1.68	1.68
Mass Boundary Roughness	0.43	0.48	0.59	0.47
Mean Radial Distance	0.49	0.50	0.07	0.07
Radial Distance Standard Deviation	0.24	0.25	0.03	0.02
Zero Crossing Count	30.60	10.03	24.82	6.65
Bounded Ellipsoid Volume Ratio	0.44	0.55	0.09	0.08
Major Angle	0.81	-0.08	2.68	2.68
Intermediate Angle	-0.16	-0.13	0.61	0.65
Minor Angle	-0.34	-0.11	1.43	1.34
Sphericity	0.54	0.69	0.10	0.07
Spherical Disproportion	1.93	1.46	0.45	0.18

The p-value, hazard ratio (HR) and its 95% confidence interval (CI), and Wald statistic value (w) obtained from the univariate Cox regression analysis for the shape features obtained for the FLAIR and T1CE masks are shown in Table 2. Shape features with p-value < 0.05 are considered to be significant for prognosis of OS in GBM patients. The HR and its 95% CI, and w values were also considered to decide whether a feature is significant. BEVR, sphericity and spherical disproportion derived from both FLAIR and T1CE masks were found to be significant for OS prognosis in GBM patients.

Table 2
Univariate Cox regression analysis results for the shape features obtained from the FLAIR and T1CE mask are shown here.

FLAIR mask			
Features	HR (95% CI)	w	p-value
Area Ratio	0.69 (0.003–160)	0.02	0.89
Mass Circularity	1 (1–1)	5.6	0.017
Entropy of radial distance	1.2 (1–1.4)	4.6	0.033
Mass Boundary Roughness	0.75 (0.47–1.2)	1.4	0.24
Mean Radial Distance	0.26 (0.0099–6.6)	0.68	0.41
Radial Distance Standard Deviation	0.00094 (1e-07-8.6)	2.2	0.13
Zero Crossing Count	1 (1–1)	6	0.014
Bounded Ellipsoid Volume Ratio*	0.017 (0.001–0.28)	8.1	0.0044
Major Angle	1 (0.96–1.1)	0.87	0.35
Intermediate Angle	1.1 (0.73–1.7)	0.2	0.65
Minor Angle	0.99 (0.84–1.2)	0.03	0.87
Sphericity*	0.052 (0.0049–0.55)	6	0.014
Spherical Disproportion*	1.9 (1.2–3.1)	6.5	0.011
T1CE mask			
Features	HR (95% CI)	w	p-value
Area Ratio	1.2 (0.0045–310)	0	0.95
Mass Circularity	1.1 (1–1.1)	6.7	0.0098
Entropy of radial distance	1.1 (0.97–1.4)	2.5	0.11
Mass Boundary Roughness	0.97 (0.56–1.7)	0.01	0.93
Mean Radial Distance	1.1 (0.032–38)	0	0.95
Radial Distance Standard Deviation	1.6 (0.00018–15000)	0.01	0.92
Zero Crossing Count	1 (1–1.1)	3	0.081
Bounded Ellipsoid Volume Ratio*	0.0016 (5.3e-05-0.049)	14	0.00023
Major Angle	1.1 (0.96–1.2)	1.2	0.27
Intermediate Angle	0.92 (0.64–1.3)	0.22	0.64
Minor Angle	0.96 (0.8–1.2)	0.14	0.7
Sphericity*	0.0054 (0.00018–0.16)	9.1	0.0025
Spherical Disproportion*	7.1 (2.1–24)	9.9	0.0017

The features found significant based on their p-value, Wald statistic value (w), hazard ratio (HR) and its 95% confidence interval (CI) are marked with *. The multivariate Cox regression analysis was performed for the features found to be significant from the univariate Cox regression analysis, with age and KPS as covariates. The results are shown in Table 3.

Table 3

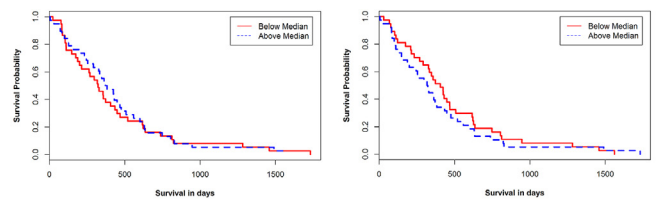
The KM survival curves obtained from the FLAIR and T1CE masks for all the shape features are shown in Fig. 3.

Features	FLAIR mask		T1CE Mask	
	w	p-value	w	p-value
Bounded Ellipsoid Volume Ratio	17.05	0.000691	19.07	0.000265
Sphericity	15	0.00181	16.49	0.0009
Spherical Disproportion	15.18	0.00167	17.4	0.000583

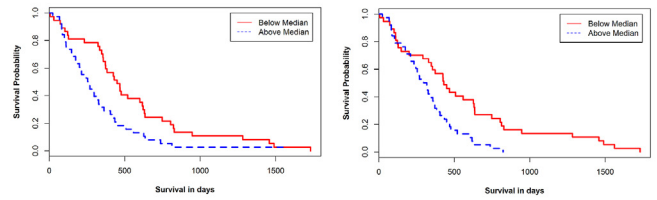
The p-value and Wald statistic value (w) from the multivariate Cox regression performed for the features found to be significant from Table 2 are shown here. The multivariate Cox regression was carried out by combining the features found significant from univariate Cox regression with clinical features: age and KPS.

extraction of large amount of quantitative features (called radiomic features) from medical images for obtaining certain inferences. The radiomics research attempts at predicting disease prognosis and therapeutic response, thus providing beneficial information for personalized treatment from a variety of imaging features extracted from multiple MR images.

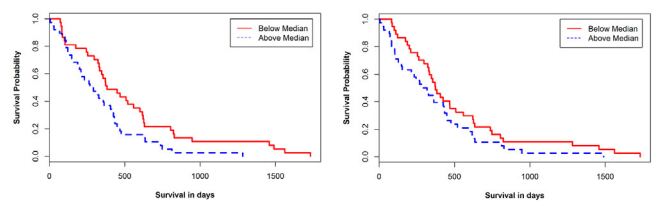
The existing literature shows that there has been an extensive study to investigate features that are prognostic of OS in GBM patients. Initially, the investigations were carried out using clinical features like age, KPS and extent of resection [1]. Eventually, the use of pre-operative MRI features for OS prognosis studies gained momentum [24]. Tumor volumetric features were used first and gradually, researchers started investigating tumor texture features for this purpose [10,25–27]. Only recently, tumor shape features were explored for OS



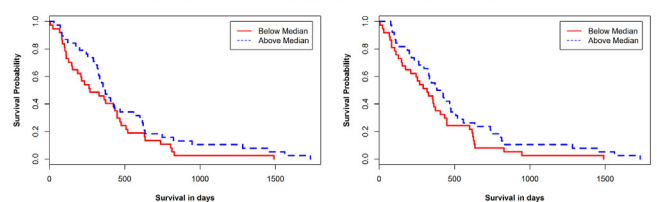
(a) Kaplan-Meier plots for Area Ratio shape feature obtained from the FLAIR (left) and T1CE (right) masks respectively



(b) Kaplan-Meier plots for Mass Circularity shape feature obtained from the FLAIR (left) and T1CE (right) masks respectively



(c) Kaplan-Meier plots for Entropy of Radial Distance shape feature obtained from the FLAIR (left) and T1CE (right) masks respectively



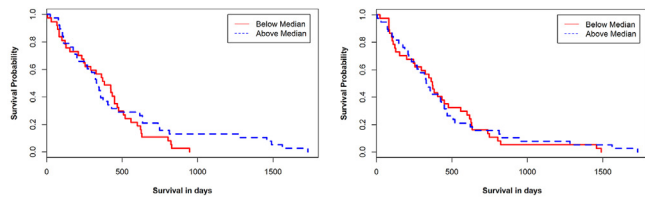
(d) Kaplan-Meier plots for Mass Boundary Ratio shape feature obtained from the FLAIR (left) and T1CE (right) masks respectively

Fig. 3. Kaplan-Meier survival plots are shown for the all the shape features computed from the FLAIR and T1CE masks.

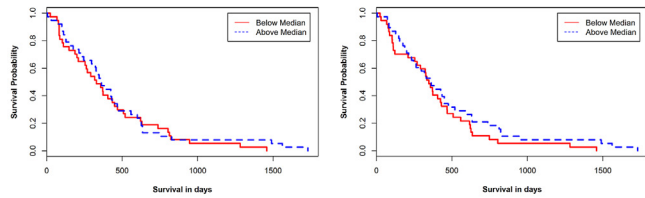
prognosis [28,29]. The study by Chaddad et al. uses only 2D shape features, whereas the study by Mazurowski et al. incorporated one 3D shape feature for OS prediction of GBM patients.

In our study, we assessed 2D as well as 3D shape features derived from FLAIR and T1CE abnormality region masks for OS prognosis using Cox regression and Kaplan-Meier survival analysis. This is the first study where tumor shape features like sphericity, spherical disproportion and certain 2D shape features were analyzed for OS prognosis and prediction of GBM patients.

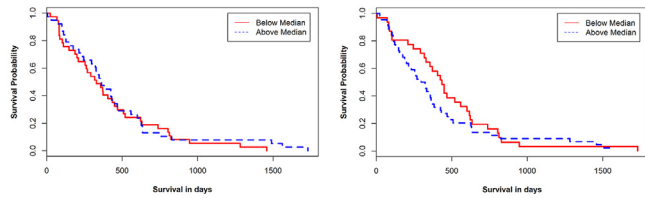
From Table 2, it was observed that only BEVR, sphericity and spherical disproportion derived from the FLAIR mask were significant prognostic indicators of survival in GBM patients with p-values 0.0044, 0.014 and 0.011 respectively. Mass circularity, entropy of radial distance and zero crossing count had p-values < 0.05. However, the 95% CI of their HR included the value 1.0. HR value of 1.0 indicates that the OS prognosis by that feature is poor. Hence, these features were not considered to be significant. BEVR, sphericity and spherical disproportion extracted from the T1CE mask where found to be significant, as they had p-value < 0.05 (refer Table 2). Although mass circularity and zero crossing had p-value < 0.05, they were not considered to be significant as the 95% CI of their HR included the value 1.0.



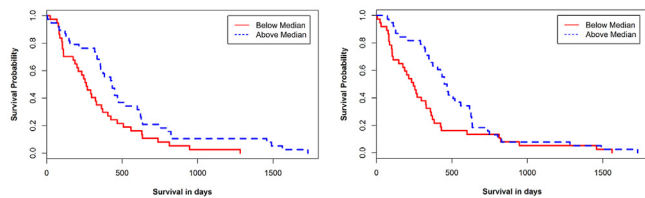
(e) Kaplan-Meier plots for Mean Radial Distance shape feature obtained from the FLAIR (left) and T1CE (right) masks respectively



(f) Kaplan-Meier plots for Radial Distance Standard Deviation shape feature obtained from the FLAIR (left) and T1CE (right) masks respectively



(g) Kaplan-Meier plots for Zero Crossing Count shape feature obtained from the FLAIR (left) and T1CE (right) masks respectively



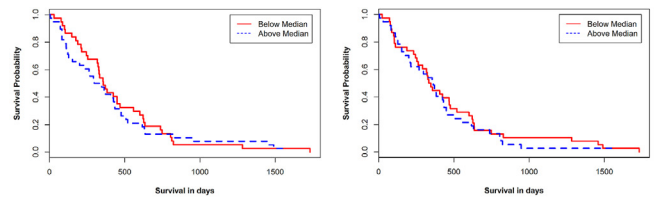
(h) Kaplan-Meier plots for Bounded Ellipsoid Volume Ratio shape feature obtained from the FLAIR (left) and T1CE (right) masks respectively

Fig. 3. (continued)

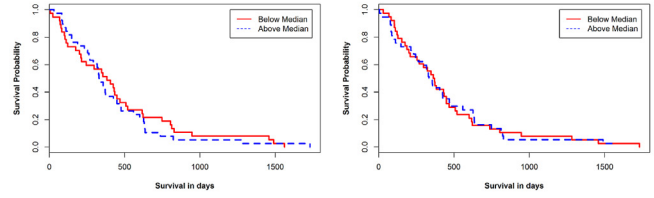
It was observed that no 2D shape feature obtained from the FLAIR and T1CE masks were significant for OS prognosis in GBM patients from the univariate Cox regression analysis (refer Table 2). However, the 3D shape features BEVR, sphericity and spherical disproportion computed from both FLAIR and T1CE masks were found to be significant. For all the three features, p-values < 0.05 and high Wald statistic values were obtained.

From both univariate and multivariate Cox regression analysis, higher Wald statistic value and lower p-values of the significant features computed from the T1CE mask were observed as compared to those obtained from the FLAIR mask. This indicates that the significant shape features computed from the T1CE mask were more effective for OS prognosis in GBM patients, compared to the shape features computed from the FLAIR mask.

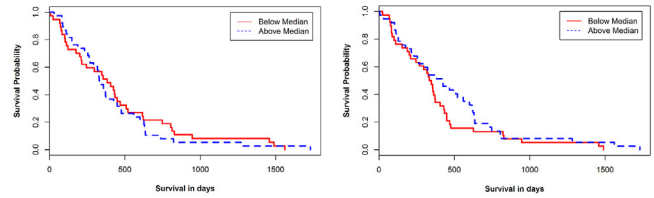
KM plots for all the shape features computed from the FLAIR and T1CE masks were observed to illustrate their effectiveness in OS prognosis. For each shape feature, two patient groups were generated based on the median value of the feature in consideration. Subsequently, the survival curve for each group was observed. Fig. 3 illustrates that the shape features found to be insignificant for OS prediction from the univariate and multivariate Cox regression showed very little or no distinction in the two curves representing the groups



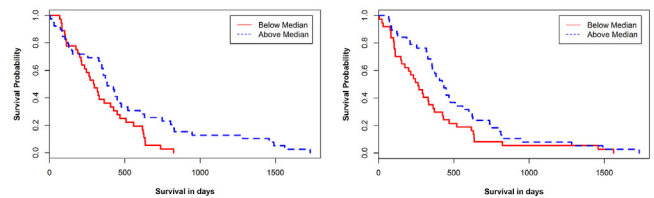
(i) Kaplan-Meier plots for Major Angle shape feature obtained from the FLAIR (left) and T1CE (right) masks respectively



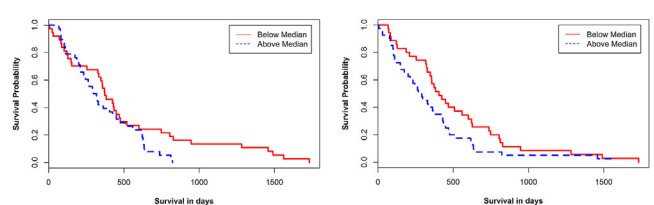
(j) Kaplan-Meier plots for Intermediate Angle shape feature obtained from the FLAIR (left) and T1CE (right) masks respectively



(k) Kaplan-Meier plots for Minor Angle shape feature obtained from the FLAIR (left) and T1CE (right) masks respectively



(l) Kaplan-Meier plots for Sphericity shape feature obtained from the FLAIR (left) and T1CE (right) masks respectively



(m) Kaplan-Meier plots for Spherical Disproportion shape feature obtained from the FLAIR (left) and T1CE (right) masks respectively

Fig. 3. (continued)

above and below their median values. This implies that there was no significant difference in the survival probability of the feature group above and below the median value. On the contrary, a clear separation between the two groups (above and below median value) was observed for the three shape features found to be significant for overall survival prediction. High BEVR and sphericity values indicate that the tumor has less irregularities. Hence, GBM patients whose tumor masks have BEVR and sphericity values above the median value for the population are expected to have higher survival probability compared to the other group. The observations from Fig. 3 for BEVR and sphericity confirms this. On the other hand, low spherical disproportion value indicates that

the tumor shape has less irregularities. Hence, GBM patients whose tumor masks have spherical disproportion value below the median value for the population are expected to survive longer. The observations from Fig. 3 for spherical disproportion confirms this.

The results from this study show that an irregular tumor shape signifies poor survival, while a regular tumor surface is associated with prolonged survival.

5. Conclusion

The primary contribution of this work is the assessment of 2D and 3D shape features which have not been analyzed in the context of OS prognosis in GBM patients. The shape features obtained from both FLAIR and T1CE abnormality masks were analyzed in this study. It was found that the tumor shape features derived from the T1CE masks were more significant in OS prognosis of GBM patients, compared to the ones derived from the FLAIR mask. Although, the 2D shape features used by Georgiou et al. [17] have been shown to be effective for breast tumor analysis, they were not found to be significant for OS prognosis in GBM patients. This observation can be attributed to the fact that GBM tumors are known to be significantly different from the other tumors in terms of their growth pattern and heterogeneity. BEVR was found to be prognostic of OS in GBM patients, which is consistent with the findings by Czarnek et al. [7]. However, the orientation of the minimum volume bounding ellipsoid of the tumor was not found to be a significant feature. Sphericity and spherical disproportion were found to be prognostic of OS in GBM patients. Hence, these 3D shape features can be used for OS prediction of GBM patients in future studies.

Funding

This work is supported by the NMRC Bedside Bench under grant R-397-000-245-511 and the Singapore Ministry of Health National Medical Research Council under its Transnational and Clinical Research Flagship Program- Tier 1 (Project No: NMRC/TCR/016-NNI/2016).

Appendix A. Supplementary data

Supplementary data to this article can be found online at <https://doi.org/10.1016/j.suronc.2019.05.005>.

References

- [1] M. Lacroix, D. Abi-Said, D.R. Fourney, Z.L. Gokaslan, W. Shi, F. DeMonte, F.F. Lang, I.E. McCutcheon, S.J. Hassenbusch, E. Holland, K. Hess, C. Michael, D. Miller, R. Sawaya, A multivariate analysis of 416 patients with glioblastoma multiforme: prognosis, extent of resection, and survival, *J. Neurosurg.* 95 (2) (2001) 190–198.
- [2] V. Hakin-Smith, D. Jellinek, D. Levy, T. Carroll, M. Teo, W. Timperley, M. McKay, R. Reddel, J. Royds, Alternative lengthening of telomeres and survival in patients with glioblastoma multiforme, *The Lancet* 361 (9360) (2003) 836–838.
- [3] D.R. Johnson, B.P. O'Neill, Glioblastoma survival in the United States before and during the temozolomide era, *J. Neuro Oncol.* 107 (2) (2012) 359–364.
- [4] N. Sanai, Integrated genomic analysis identifies clinically relevant subtypes of glioblastoma, *World Neurosurgery* 74 (1) (2010) 4–5.
- [5] D. Cordier, F. Forrer, S. Kneifel, M. Sailer, L. Mariani, H. Mäcke, J. Müller-Brand, A. Merlo, Neoadjuvant targeting of glioblastoma multiforme with radiolabeled dotaga–substance results from a phase I study, *J. Neuro Oncol.* 100 (1) (2010) 129–136.
- [6] F.K. Albert, M. Forsting, K. Sartor, H.-P. Adams, S. Kunze, Early postoperative magnetic resonance imaging after resection of malignant glioma: objective evaluation of residual tumor and its influence on regrowth and prognosis, *Neurosurgery* 34 (1) (1994) 45–61.
- [7] N. Czarnek, K. Clark, K.B. Peters, M.A. Mazurkowski, Algorithmic three-dimensional analysis of tumor shape in mri improves prognosis of survival in glioblastoma: a multi-institutional study, *J. Neuro Oncol.* (2017) 1–8.
- [8] S. Drabycz, G. Roldán, P. De Robles, D. Adler, J.B. McIntyre, A.M. Magliocco, J.G. Cairncross, J.R. Mitchell, An analysis of image texture, tumor location, and mgmt promoter methylation in glioblastoma using magnetic resonance imaging, *Neuroimage* 49 (2) (2010) 1398–1405.
- [9] J. Lee, R. Jain, K. Khalil, B. Griffith, R. Bosca, G. Rao, A. Rao, Texture feature ratios from relative cbv maps of perfusion mri are associated with patient survival in glioblastoma, *Am. J. Neuroradiol.* 37 (1) (2016) 37–43.
- [10] D. Yang, G. Rao, J. Martinez, A. Veeraraghavan, A. Rao, Evaluation of tumor-derived mri-texture features for discrimination of molecular subtypes and prediction of 12-month survival status in glioblastoma, *Med. Phys.* 42 (11) (2015) 6725–6735.
- [11] A.-W. Awad, M. Karsy, N. Sanai, R. Spetzler, Y. Zhang, Y. Xu, M.A. Mahan, Impact of removed tumor volume and location on patient outcome in glioblastoma, *J. Neuro Oncol.* (2017) 1–11.
- [12] J. Simpson, J. Horton, C. Scott, W. Curran, P. Rubin, J. Fischbach, S. Isaacson, M. Rotman, S. Asbell, J. Nelson, A.S. Weinstein, D.F. Nelson, Influence of location and extent of surgical resection on survival of patients with glioblastoma multiforme: results of three consecutive radiation therapy oncology group (rtog) clinical trials, *Int. J. Radiat. Oncol. Biol. Phys.* 26 (2) (1993) 239–244.
- [13] C. Henker, T. Kriesen, A. Glass, B. Schneider, J. Piek, Volumetric quantification of glioblastoma: experiences with different measurement techniques and impact on survival, *J. Neuro Oncol.* (2017) 1–12.
- [14] N. Sanai, M.S. Berger, Glioma extent of resection and its impact on patient outcome, *Neurosurgery* 62 (4) (2008) 753–766.
- [15] N. Sanai, M.-Y. Polley, M.W. McDermott, A.T. Parsa, M.S. Berger, An extent of resection threshold for newly diagnosed glioblastomas, *J. Neurosurg.* 115 (1) (2011) 3–8.
- [16] J. van Griethuysen, A. Fedorov, C. Parmar, A. Hosny, N. Aucoin, V. Narayan, R. Beets-Tan, J. Fillion-Robin, S. Pieper, H. Aerts, Computational radiomics system to decode the radiographic phenotype, *Cancer research* 77 (21) (2017) e104–e107.
- [17] H. Georgiou, M. Mavroforakis, N. Dimitropoulos, D. Cavouras, S. Theodoridis, Multi-scaled morphological features for the characterization of mammographic masses using statistical classification schemes, *Artif. Intell. Med.* 41 (1) (2007) 39–55.
- [18] S. Bakas, H. Akbari, A. Sotiras, M. Bilello, M. Rozycki, J.S. Kirby, J.B. Freymann, K. Farahani, C. Davatzikos, Advancing the cancer genome atlas glioma mri collections with expert segmentation labels and radiomic features, *Sci. Data* 4 (2017) sdata2017117.
- [19] S. Bakas, H. Akbari, A. Sotiras, M. Bilello, M. Rozycki, J. Kirby, J. Freymann, K. Farahani, C. Davatzikos, Segmentation Labels and Radiomic Features for the Pre-operative Scans of the Tcga-Lgg Collection, *The Cancer Imaging Archive*.
- [20] M. Kistler, S. Bonaretti, M. Pfahrer, R. Niklaus, P. Büchler, The virtual skeleton database: an open access repository for biomedical research and collaboration, *J. Med. Internet Res.* 15 (11) (2013) e245.
- [21] B.H. Menze, A. Jakab, S. Bauer, J. Kalpathy-Cramer, K. Farahani, J. Kirby, Y. Burren, N. Porz, J. Slotboom, R. Wiest, L. Lanczi, E. Gerstner, M.-A. Weber, T. Arbel, B.B. Avants, N. Ayache, P. Buendia, D.L. Collins, N. Cordier, J.J. Corso, A. Criminisi, T. Das, H. Delingette, C. Demiralp, C.R. Durst, M. Dojat, S. Doyle, J. Festa, F. Forbes, E. Geremia, B. Glocker, P. Golland, X. Guo, A. Hamamci, K.M. Iftekharuddin, R. Jena, N.M. John, E. Konukoglu, D. Lashkari, J.A. Mariz, R. Meier, S. Pereira, D. Precup, S.J. Price, T.R. Raviv, S.M.S. Reza, M. Ryan, D. Sarikaya, L. Schwartz, H.-C. Shin, J. Shotton, C.A. Silva, N. Sousa, N.K. Subbanna, G. Szekely, T.J. Taylor, O.M. Thomas, N.J. Tustison, G. Unal, F. Vasseur, M. Wintermark, D.H. Ye, L. Zhao, B. Zhao, D. Zikic, M. Prastawa, M. Reyes, K.V. Leemput, The multimodal brain tumor image segmentation benchmark (brats), *IEEE Trans. Med. Imaging* 34 (10) (2015) 1993–2024.
- [22] N. Moshtagh, Minimum volume enclosing ellipsoid, *Convex Optim.* 111 (2005) 112.
- [23] S. Bektas, Least squares fitting of ellipsoid using orthogonal distances, *Bol. Ciências Geodésicas* 21 (2) (2015) 329–339.
- [24] M.A. Hammoud, R. Sawaya, W. Shi, P.F. Thall, N.E. Leeds, Prognostic significance of preoperative mri scans in glioblastoma multiforme, *J. Neuro Oncol.* 27 (1) (1996) 65–73.
- [25] M.A. Mazurkowski, J. Zhang, K.B. Peters, H. Hobbs, Computer-extracted mr imaging features are associated with survival in glioblastoma patients, *J. Neuro Oncol.* 120 (3) (2014) 483–488.
- [26] A. Chaddad, S. Sabri, T. Niazi, B. Abdulkarim, Prediction of survival with multi-scale radiomic analysis in glioblastoma patients, *Med. Biol. Eng. Comput.* 56 (12) (2018) 2287–2300.
- [27] A. Chaddad, P. Daniel, C. Desrosiers, M. Toews, B. Abdulkarim, Novel radiomic features based on joint intensity matrices for predicting glioblastoma patient survival time, *IEEE J. Biomed. Health Inf.* 23 (2) (2019) 795–804 Mar.
- [28] A. Chaddad, C. Desrosiers, L. Hassan, C. Tanougast, A quantitative study of shape descriptors from glioblastoma multiforme phenotypes for predicting survival outcome, *Br. J. Radiol.* 89 (1068) (2016) 20160575.
- [29] M.A. Mazurkowski, N.M. Czarnek, L.M. Collins, K.B. Peters, K. Clark, Predicting outcomes in glioblastoma patients using computerized analysis of tumor shape: preliminary data, *Medical Imaging 2016: Computer-Aided Diagnosis*, vol. 9785, International Society for Optics and Photonics, 2016, p. 97852T.